Electronic Supplementary Material (ESI) for Journal of Materials Chemistry A.
This journal is © The Royal Society of Chemistry 2021

Supporting Information

Graphene-quantum-dot-composited platinum nanotube arrays as a dual efficient electrocatalyst for the oxygen reduction reaction and methanol electro-oxidation

Lili Zhang,[a] Panpan Lu,[a] Yaru Luo,[b] Jin You Zheng,[a] Wei Ma,*[a] Liang-Xin Ding *[b] and Haihui Wang *[c]

[a] Engineering Research Center of Advanced Functional Material Manufacturing of Ministry of Education, School of Chemical Engineering, Zhengzhou University, Zhengzhou 450001, China.

[b] School of Chemistry and Chemical Engineering, South China University of Technology, Guangzhou 510640, China.

[c] Beijing Key Laboratory for Membrane Materials and Engineering, Department of Chemical Engineering, Tsinghua University, Beijing 100084, China.

***Email**: mawei@zzu.edu.cn; lxding@scut.edu.cn; cehhwang@tsinghua.edu.cn.

Table of Contents

I. Supplementary Methods

Electrochemically active surface area (ECSA) calculation

CV measurements were conducted in N_2 saturated 0.5 M H_2SO_4 solution at a scan rate of 50 mV s^{-1}. The electrochemically active surface area (ECSA) of catalysts was calculated using eq.1 and eq.2:[1]

$$ECSA = Q_H/(m \times q_H) \quad (1)$$

Where Q_H is the under-potentially deposited hydrogen charge, m is the loading amount of metal, and q_H is the charge required for monolayer adsorption of hydrogen on a Pt surface, which is assumed to be 0.21 mC cm^{-2}.

$$Q_H = \int_0^{0.35} \frac{I[A] \times dE[V]}{v[V/S]} \quad (2)$$

Where I is the current, E the potential, v the scan rate.

Transfer electron numbers (*n*) calculation

ORR were test in O_2 saturated 0.1 M $HClO_4$ solution at 5 mV s^{-1}. The transfer electron numbers per oxygen molecule (*n*) in the ORR was determined by the K-L equations as follows:[2,3]

(i) $$\frac{1}{j} = \frac{1}{j_k} + \frac{1}{Bw^{1/2}} \quad (3)$$

where j is the measured current density, j_k is the kinetic current density and w is the angular velocity of the disk (w=2πN, N is the linear rotation speed).

$$B = 0.62nFC_{O_2}(D_{O_2})^{2/3}v^{-1/6} \quad (4)$$

where n represents the overall number of electrons gained per oxygen, F is the Faraday constant (F=96485 C mol^{-1}), C_{O_2} is the bulk concentration of O_2 (1.26×10^{-3}

mol L^{-1}), D_{O2} is the diffusion coefficient of O_2 in 0.1 M $HClO_4$ electrolyte (1.93×10^{-5} cm^2 s^{-1}),v is the kinetic viscosity of the electrolyte (1.009×10^{-2} cm^2 s^{-1}).

(ii) $$n = 4I_d / (I_d + I_r / N) \quad (5)$$

where I_d is the disk current, I_r is the ring current and N is the collection efficiency. The value of N was experimentally determined to be 0.37 by using a standard ferricyanide system.[4]

Density functional theory (DFT) method and model

The Pt (111), Pt (200), Pt (111) + C (101) and Pt (200) + C (101) surfaces were been built, where the vacuum space along the z direction is set to be 18 Å, which is enough to avoid interaction between the two neighboring images. Then O_2 molecule was loaded on the surface. The bottom two atomic layers were fixed, the top three atomic layers were relaxed adequately for Pt (111) and Pt (200) surfaces, and all atoms were relaxed adequately for Pt (111) + C (101) and Pt (200) + C (101) surfaces. The first principles calculations in the framework of density functional theory were carried out based on the Cambridge Sequential Total Energy Package known as CASTEP.[5] The exchange-correlation functional under the generalized gradient approximation (GGA)[6] with norm-conserving pseudopotentials and Perdew-Burke-Ernzerhof functional was adopted to describe the electron-electron interaction.[7]An energy cutoff of 750 eV was used and a k-point sampling set of 5 x 5 x 1 were tested to be converged. A force tolerance of 0.01 eV $Å^{-1}$, energy tolerance of $5.0x10^{-7}$eV per atom and maximum displacement of $5.0x10^{-4}$ Å were considered. The Grimme method for DFT-D correction is considered for all calculations.[8]

Adsorption energy ΔE of A (=O_2) molecule on the surface of substrates was defined as:[9]

$$\Delta E = E_{*A} - (E_{*} + E_{A}) \quad (6)$$

where *A and * denote the adsorption of A molecule on substrates and the bare substrates, EA denotes the energy of A molecule. The energy of O_2 gas was calculated by ($2E_{H2O}$ - $2E_{H2}$ + 4.92), since the negative of experimental energy of formation of two water molecules ($-2\Delta^{exp}_{H_2O}$ = 4.92 eV).[10]

II. Supplementary Figures

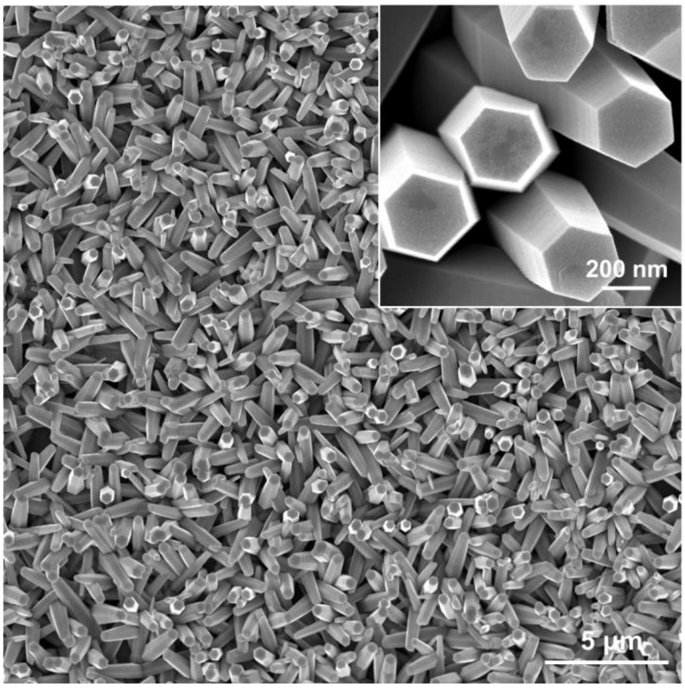

Fig. S1. SEM images of ZnO nanorod arrays.

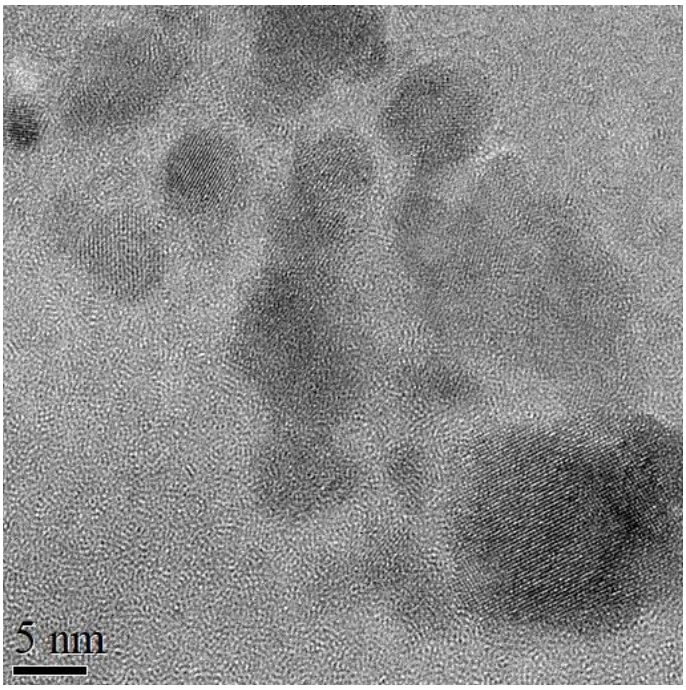

Fig. S2. TEM image of GQDs.

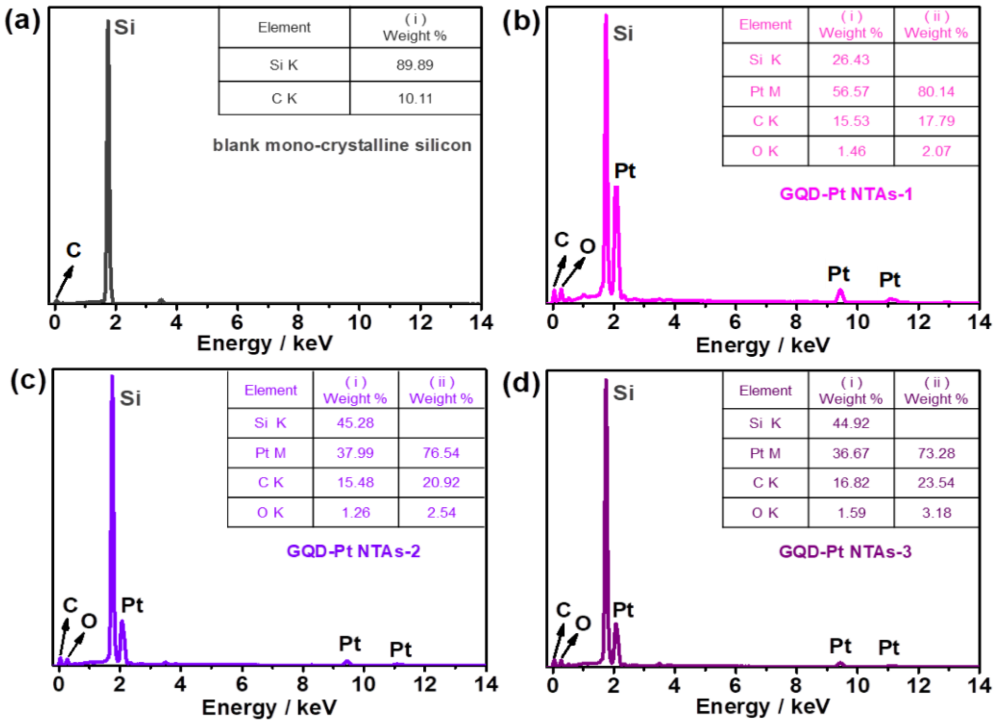

Fig. S3. SEM-EDS spectrum of (a) blank mono-crystalline silicon, (b) GQD-Pt NTAs-1, (c) GQD-Pt NTAs-2, and (d) GQD-Pt NTAs-3.

The GQD-Pt NTAs catalysts with different amounts of GQDs were obtained by electroreducing mixed solution with the ratio of 1:1, 2:1 or 4:1 for H_2PtCl_6•$6H_2O$ to GQDs, which are denoted GQD-Pt NTAs-1, GQD-Pt NTAs-2 and GQD-Pt NTAs-3, respectively. The SEM-EDS of these GQD-Pt NTAs catalysts are measured on a blank mono-crystalline silicon substrate. As shown in **Fig. S3**, (i) represents the element content of the sample and substrate, and (ii) represents the element content of the sample after removing impurities in the substrate.

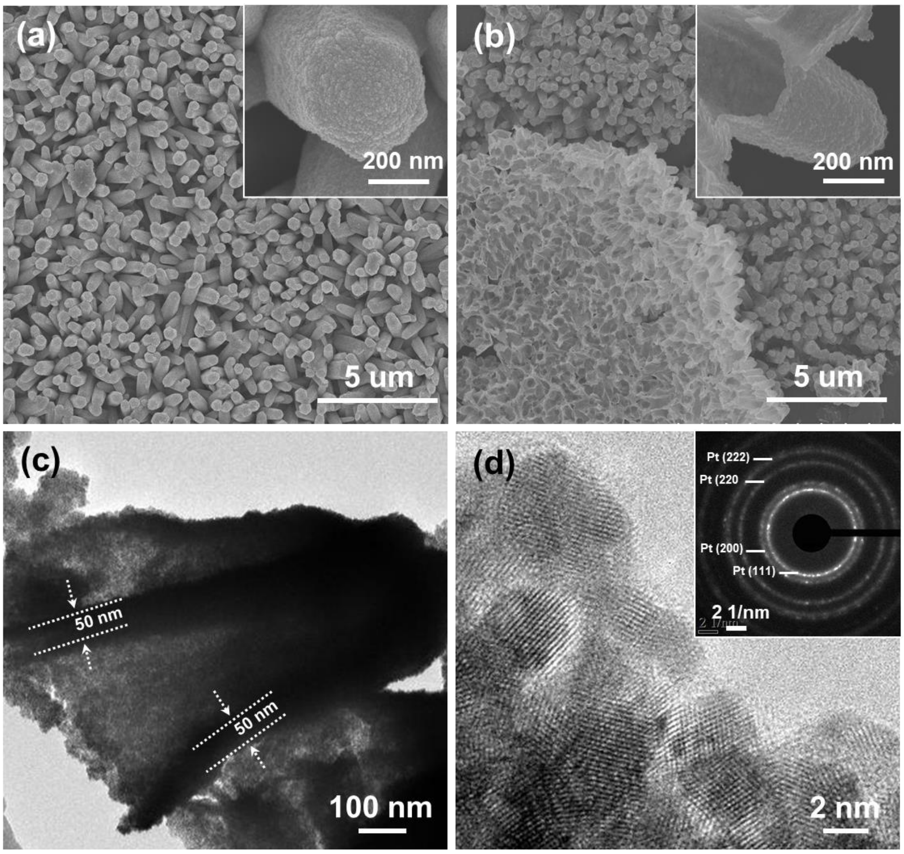

Fig. S4. SEM images of (a) ZnO@ Pt core-shell NRAs and (b) Pt NTAs. The insets in (a) and (b) are the high magnification SEM images. (c, d) TEM images and SAED pattern (inset in (d)) of typical Pt NTAs.

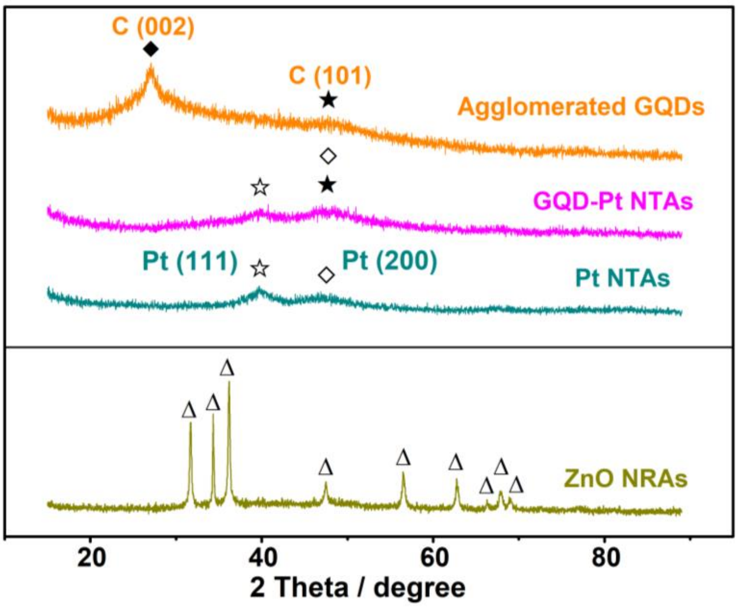

Fig. S5. XRD pattern of the as-prepared catalysts.

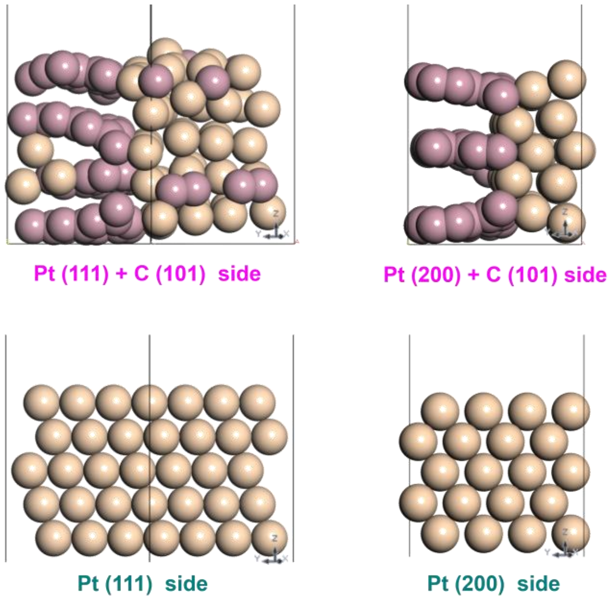

Fig. S6. Optimized structural surfaces of Pt (111) + C (101), Pt (200) + C (101), Pt (111) and Pt (200).

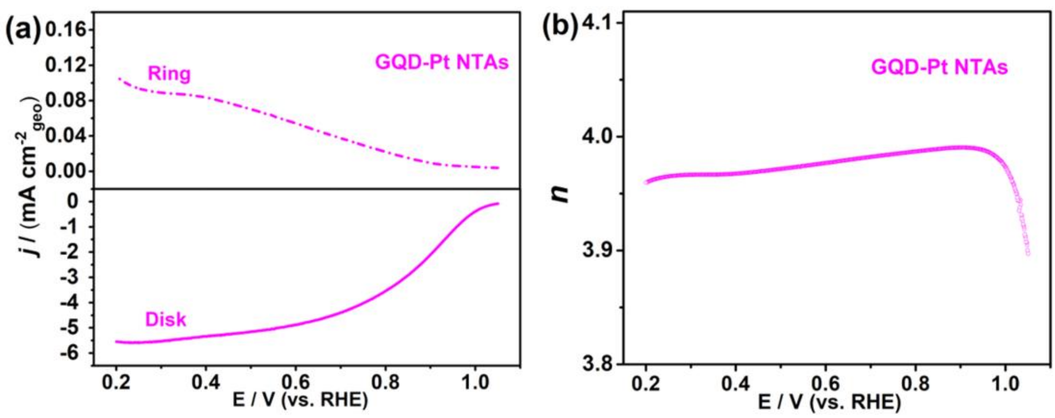

Fig. S7. RRDE technique over GQD-Pt NTAs electrocatalyst: (a) polarization curves and (b) the calculated corresponding transferred electron number (n).

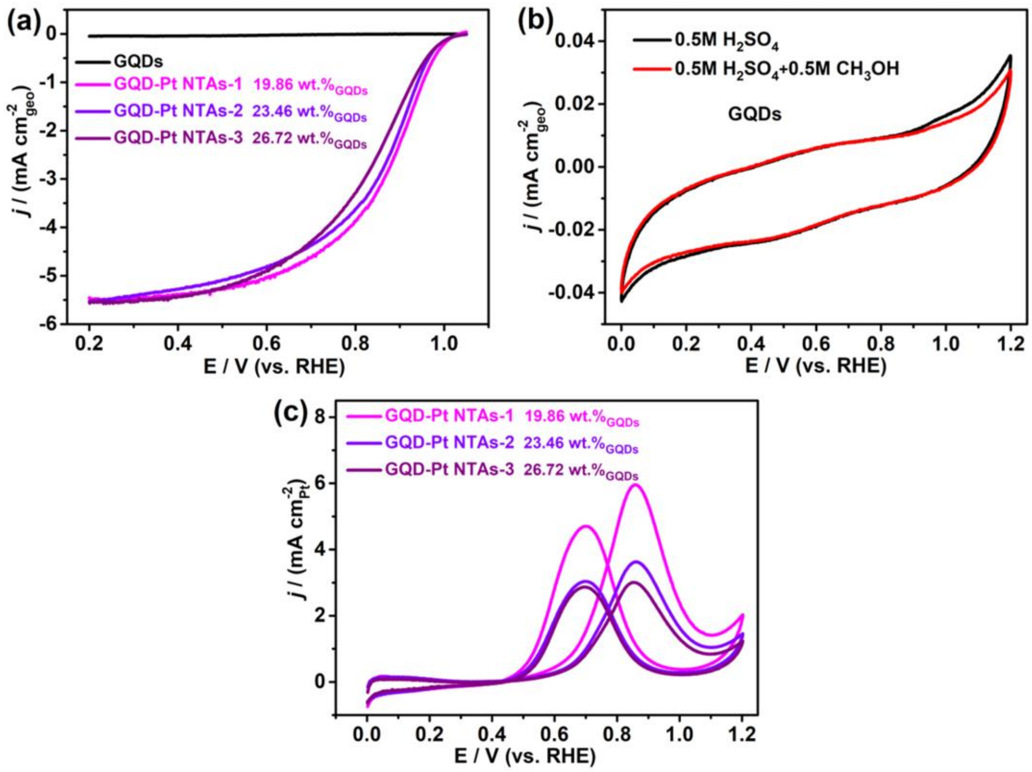

Fig. S8. (a) ORR polarization curves. (b) CVs in 0.5 M H_2SO_4 and 0.5 M CH_3OH + 0.5 M H_2SO_4 for GQDs at 50 mV s^{-1}. (c) MOR CVs for the GQD-Pt NTAs catalysts with different amounts of GQDs.

III. Supplementary Tables

Table S1. Comparison of the work function, adsorption energy (E_{abs}) and Bader charge values.

Components	Work function (eV)	E_{abs} (eV)	Bader charge (eV)
Pt (111)	-5.99	--	--
Pt (111) + C (101)	-5.23	--	--
Pt (200)	-5.84	--	--
Pt (200) + C (101)	-5.03	--	--
Pt (111) + O_2	--	-1.33	-0.30
Pt (111) + C (101) + O_2	--	-4.26	-0.45
Pt (200) + O_2	--	-2.56	-0.34
Pt (200) + C (101) + O_2	--	-5.37	-0.47

Table S2. The mass activity and specific activity of platinum-based electrocatalysts for ORR.

Catalysts	Conditions	Mass activity (mA μg $_{Pt}^{-1}$)	Specific activity (mA cm_{Pt}^{-2})	Reference
GQD-Pt NTAs	**0.1M $HClO_4$ (0.9 V vs. RHE)**	**1.14**	**2.24**	**This work**
PtCo NCs	0.1M $HClO_4$ (0.9 V vs. RHE)	1.65	1.85	11
Pt@holey rGO@Pt	0.5M H_2SO_4 (0.85 V vs. RHE)	0.60	2.12	12
PtNiPb NPs	0.1M $HClO_4$ (0.9 V vs. RHE)	0.449	0.976	13
$FePtCe_1/C$	0.5M H_2SO_4 (0.9 V vs. RHE)	0.734	3.38	14
$Pt_{71}Co_{29}$ LNFs	0.1M $HClO_4$ (0.75 V vs. RHE)	0.128	0.43	15
Pd_1Pt_4 DNSs	0.1M $HClO_4$ (0.9 V vs. RHE)	0.53	0.74	16

PtPd SAANs	0.1M $HClO_4$ (0.8 V vs. RHE)	2.75	0.95	17
PtBi nanoplates/C	0.1M $HClO_4$ (0.9 V vs. RHE)	0.353	1.04	18
Au/CuPt	0.1M $HClO_4$ (0.9 V vs. RHE)	1.7	2.75	19
AuNP@PANI@PtFe	0.1M $HClO_4$ (0.8 V vs. RHE)	0.43	2.73	20
PtCo/C	0.1M $HClO_4$ (0.8 V vs. RHE)	0.237	0.439	21
PtNiRh trimetallic NWs/C	0.1M $HClO_4$ (0.9 V vs. RHE)	2.88	2.71	22
PtPdNiP MNs	0.1M $HClO_4$ (0.9 V vs. RHE)	0.45	0.89	23
H-PtNiCu-AAT NPs	0.1M $HClO_4$ (0.9 V vs. RHE)	0.977	1.458	24
Pt-Co/C	0.1M $HClO_4$ (0.9 V vs. RHE)	0.64	1.29	25
Pt/p-BN	0.1M $HClO_4$ (0.9 V vs. RHE)	1.06	1.24	26
37 wt%-FePt/rGO	0.1M $HClO_4$ (0.9 V vs. RHE)	1.96	4.1	27
Pt/RGO/CB-1	0.1M $HClO_4$ (0.9 V vs. RHE)	0.109	0.212	28
APD-Pt/needles-GC	0.1M $HClO_4$ (0.9 V vs. RHE)	0.62	1.3	29

Table S3. The mass activity and specific activity of platinum-based electrocatalysts for MOR.

Catalysts	Conditions	Mass activity (mA mg $_{Pt}^{-1}$)	Specific activity (mA cm_{Pt}^{-2})	Reference
GQD-Pt NTAs	**0.5M H_2SO_4 +0.5M CH_3OH**	**2227.08**	**5.95**	**This work**
PtCo NCs	0.5M H_2SO_4	514.5	2.57	11

	+0.5M CH_3OH			
Pt@holey rGO@Pt	0.5M H_2SO_4 +0.5M CH_3OH	575.2	1.05	12
PtNiPb NPs	0.1M $HClO_4$ +0.5M CH_3OH	1160	2.40	13
$FePtCe_1/C$	0.1M $HClO_4$ +0.5M CH_3OH	1018.6	1.141	14
$Pt_{71}Co_{29}$ LNFs	0.1M $HClO_4$ +0.5M CH_3OH	666.23	2.51	15
Pd_1Pt_4 DNSs	0.1M $HClO_4$ +0.5M CH_3OH	1660	2.23	16
PtPd SAANs	0.5M H_2SO_4 +0.5M CH_3OH	375.99	1.30	17
PtBi nanoplates/C	0.1M $HClO_4$ +0.1M CH_3OH	1100	3.18	18
Au/CuPt	0.1M $HClO_4$ +0.1M CH_3OH	441	0.71	19
AuNP@PANI@PtFe	0.1M $HClO_4$ +0.1M CH_3OH	913	28	20
PtCo/C	0.1M $HClO_4$ +1M CH_3OH	2110	3.62	21
Pt-WP-CL/AEG-3	0.5M H_2SO_4 +1M CH_3OH	2217	1.80	30
H-PtNiCu-AAT NPs	0.1M H_2SO_4 +1M CH_3OH	1875	2.798	24
$Pt/TiO_2/rGO$	0.5M $HClO_4$ +0.5M CH_3OH	698.9	1.24	31
$Pt_XFe/C/N$-GC-800	0.1M H_2SO_4 +1M CH_3OH	295.63	1.12	32
RGO/Pt-Pd	0.5M $HClO_4$ +1M CH_3OH	1419.6	15.6	33
$Ni_{0.20}Pt_{0.80}$ nanoflowers	0.5M H_2SO_4 +1M CH_3OH	2200	4.15	34
PtCo@NC	0.1M H_2SO_4 +1M CH_3OH	2300	5.14	35

IV. References

1 J. N. Tiwari, K. C. Kemp, K. Nath, R. N. Tiwari, H.-G. Nam and K. S. Kim, *ACS Nano*, 2013, **7**, 9223-9231.

2 M. Shao, T. Huang, P. Liu, J. Zhang, K. Sasaki, M. Vukmirovic and R. Adzic, *Langmuir*, 2006, **22**, 10409-10415.

3 V. Stamenković, T. J. Schmidt, P. N. Ross and N. M. Marković, *J. Electroanal. Chem.*, **2003**, 554-555, 191-199.

4 Z. Zheng, Y. H. Ng, D.-W. Wang and R. Amal, *Adv. Mater.*, 2016, **28**, 9949-9955.

5 M. D. Segall, P. J. D. L. M. J. Probert, C. J. Pickard, P. J. Hasnip, S. J. Clark and M. C. Payne, *J. Phys.: Condens. Matter*, 2002, **14**, 2717-2744.

6 J. P. Perdew, K. Burke and M. Ernzerhof, *Phys. Rev. Lett.*, 1996, **77**, 3865.

7 D. R. Hamann, M. Schl¨ uter and C. Chiang, *Phys. Rev. Lett.*, 1979, **43**, 1494-1497.

8 S. Grimme, *J. Comput. Chem.*, 2006, **27**, 1787-1799.

9 Y. Li, Q. Zhang, C. Li, H.-N. Fan, W.-B. Luo, H.-K. Liu and S.-X. Dou, *J. Mater. Chem. A*, 2019, **7**, 22242-22247.

10 Y. Wu, C. Li, W. Liu, H.H. Li, Y. Y. Gong, L. Y. Niu, X. J. Liu, C. Q, Sun and S. Q. Xu, *Nanoscale*, 2019, **11**, 5064-5071.

11 Q. Chen, Z. Cao, G. Du, Q. Kuang, J. Huang, Z. Xie and L. Zheng, *Nano Energy*, 2017, **39**, 582-589.

12 X. Qiu, X. Yan, K. Cen, D. Sun, L. Xu and Y. Tang, *ACS Appl. Energy Mater.*, 2018, **1**, 2341-2349.

13 N. Cheng, L. Zhang, H. Jiang, Y. Zhou, S. Yu, L. Chen, H. Jiang and C. Li, *Nanoscale*, 2019, **11**, 16945-16953.

14 J. Ma, X. Tong, J. Wang, G. Zhang, Y. Lv, Y. Zhu, S. Sun, Y.-C. Yang and Y. Song, *Electrochim. Acta*, 2019, **299**, 80-88.

15 L. Zhang, X.-F. Zhang, X.-L. Chen, A.-J. Wang, D.-M. Han, Z.-G. Wang and J.-J. Feng, *J. Colloid Interface Sci.*, 2019, **536**, 556-562.

16 X. Peng, D. Lu, Y. Qin, M. Li, Y. Guo and S. Guo, *ACS Appl. Mater. Interfaces*,

2020, **12**, 30336-30342.

17 Y.-C. Shi, L.-P. Mei, A.-J. Wang, T. Yuan, S.-S. Chen and J.-J. Feng, *J. Colloid Interface Sci.*, 2017, **504**, 363-370.

18 Y. Qin, M. Luo, Y. Sun, C. Li, B. Huang, Y. Yang, Y. Li, L. Wang and S. Guo, *ACS Catal.*, 2018, **8**, 5581-5590.

19 X. Sun, D. Li, Y. Ding, W. Zhu, S. Guo, Z. L. Wang and S. Sun, *J. Am. Chem. Soc.*, 2014, **136**, 5745-5749.

20 J.-E. Lee, Y. J. Jang, W. Xu, Z. Feng, H.-Y. Park, J. Y. Kim and D. H. Kim, *J. Mater. Chem. A*, 2017, **5**, 13692-13699.

21 Y. Ma, L. Yin, T. Yang, Q. Huang, M. He, H. Zhao, D. Zhang, M. Wang and Z. Tong, *ACS Appl. Mater. Interfaces*, 2017, **9**, 36164-36172.

22 K. Li, X. Li, H. Huang, L. Luo, X. Li, X. Yan, C. Ma, R. Si, J. Yang and J. Zeng, *J. Am. Chem. Soc.*, 2018, **140**, 16159-16167.

23 C. Li, Y. Xu, K. Deng, S. Yin, Z. Wang, H. Xue, X. Li, L. Wang and H. Wang, *J. Mater. Chem. A*, 2019, **7**, 3910-3916.

24 D. Wu, W. Zhang, A. Lin and D. Cheng, *ACS Appl. Mater. Interfaces*, 2020, **12**, 9600-9608.

25 W. Lei, M. Li, L. He, X. Meng, Z. Mu, Y. Yu, F. M. Ross and W. Yang, *Nano Research*, 2020, **13**, 638-645.

26 Q. Li, L. Li, X. Yu, X. Wu, Z. Xie, X. Wang, Z. Lu, X. Zhang, Y. Huang and X. Yang, *Chem. Eng. J.*, 2020, **399**, 125827.

27 T. Y. Yoo, J. M. Yoo, A. K. Sinha, M. S. Bootharaju, E. Jung, H. S. Lee, B.-H. Lee, J. Kim, W. H. Antink, Y. M. Kim, J. Lee, E. Lee, D. W. Lee, S.-P. Cho, S. J. Yoo, Y.-E. Sung and T. Hyeon, *J. Am. Chem. Soc.*, 2020, **142**, 14190-14200.

28 Y. Li, Y. Li, E. Zhu, T. McLouth, C.-Y. Chiu, X. Huang and Y. Huang, *J. Am. Chem. Soc.*, 2012, **134**, 12326-12329.

29 X. Zhao, Y. Hamamura, Y. Yoshida, T. Kaneko, T. Gunji, S. Takao, K. Higashi, T. Uruga and Y. Iwasawa, *ACS Appl. Energy Mater.*, 2020, **3**, 5542-5551.

30 C. Zhang, Y. Dai, H. Chen, Y. Ma, B. Jing, Z. Cai, Y. Duan, B. Tang and J. Zou, *J.*

Mater. Chem. A, 2018, **6**, 22636-22644.

31 S. Wu, J. Liu, Y. Ye, Z. Tian, X. Zhu and C. Liang, *ACS Appl. Energy Mater.*, 2019, **2**, 5577-5583.

32 J. Zhao, H. Huang, M. Liu, J.-H. Wang, K. Liu and Z.-Y. Li, *RSC Advances*, 2019, **9**, 26450-26455.

33 M. F. R. Hanifah, J. Jaafar, M. H. D. Othman, A. F. Ismail, M. A. Rahman, N. Yusof, F. Aziz and N. A. A. Rahman, *J. Alloys Compd.*, 2019, **793**, 232-246.

34 A. Shan, S. Huang, H. Zhao, W. Jiang, X. Teng, Y. Huang, C. Chen, R. Wang and W.-M. Lau, *Nano Research*, 2020, **13**, 3088-3097.

35 G. Hu, L. Shang, T. Sheng, Y. Chen and L. Wang, *Adv. Funct. Mater.*, 2020, **30**, 2002281.